Modelling of the Influence of Vegetative Barrier on Concentration of PM10 from Highway

Hynek Řezníček, Luděk Beneš

Department of Technical Mathematics, FME - Czech Technical University in Prague, Karlovo nám. 293/13, 121 35 Praha 2, Czech Republic, CR

E-mail: `hynek.reznicek@fs.cvut.cz, benes@marian.fsik.cvut.cz`

Abstract. The influence of different types of the vegetative barrier near a highway on dustiness was studied. Transport and dispersion of pollutants PM10 emitted from the highway was numerically simulated. Mathematical model was based on the Navier-Stokes equations for turbulent fluid flow in Boussinesq approximation. The AUSM-MUSCL scheme in finite volume formulation on structured orthogonal grid was used. The influence of the shape of the barrier and of its obstructing properties on the concentration of pollutants was studied.

1. Introduction

The pollution in the Atmospheric Boundary Layer (ABL) is increasing these days and its different effects on human life are more investigated. The numerical modelling can help us to predict the transmission of the pollution and to understand its behaviour. Although there are a lot of models for concentration, the core of this problem lies in a accurate fluid flow modelling. The dangerous areas can be easily identified from exact simulation of the velocity field and density distribution. Examined problems cover the research field of micrometeorology [1].

One of the problem is the increasing of car traffic on highways. The concentration of dust produced (or swirled) by the traffic is increasing as well. Therefore areas around these highways are more threatened with the dust. Some examples of increased concentration effects are the effect on human health (respiratory problems), the effects affecting the environment and the effect on agriculture. Although some solid barriers are installed near highway, it shows that there are not quite effective to prevent these effects.

The simple mathematical model of incompressible stratified fluid flow based on Navier-Stokes equations was used in 2D. The Blackadar algebraic turbulent model [2] was added and its effects were observed. The vegetative barrier was study in this paper, especially there effect on simulated fluid flow were investigated. The barrier was simulated as a rectangle with different aerodynamic obstructing force.

2. Mathematical model

This section describes in detail development and simplification of the mathematical model for incompressible fluid flow with variable density. Necessary assumptions and approximations are introduced

2.1. Simple incompressible model

The air flow in ABL is described by RANS (Reynolds Averaged Navier-Stokes) equations for the viscous, incompressible, turbulent and stratified flow with variable density (in general). The heat transfer is not considered. The system of equations is simplified with Boussinesq approximation, in 2D it is written:

$$\frac{\partial u_j}{\partial x_j} = 0,$$

$$\frac{\partial \rho}{\partial t} + \frac{\partial u_j \rho}{\partial x_j} = u_2 \frac{\partial \rho_0}{\partial x_2} \tag{1}$$

$$\frac{\partial u_i}{\partial t} + \frac{\partial u_j u_i}{\partial x_j} + \frac{1}{\rho_0} \frac{\partial p}{\partial x_i} = \frac{\partial}{\partial x_j} \nu \left(\frac{\partial u_i}{\partial x_j} \right) - \frac{\rho}{\rho_0} g \delta_{i2} + T_i,$$

where u_i ($i \in \{1,2\}$) are velocity components, ρ resp. p are perturbations of density resp. pressure, ρ_0 is background density and T_i is the aerodynamic resistance of the barrier. The viscosity was composed from the molecular kinematic viscosity and the turbulent viscosity $\nu = \nu_m + \nu_T$.

2.2. Turbulence model

The turbulent viscosity was computed from Blackadar algebraic turbulent model (see [3], [2]).

$$\nu_T = l^2 \left| \frac{\partial u_1}{\partial x_2} \right| \mathcal{G}, \tag{2}$$

where $\mathcal{G}$ is function of Richardson number Ri

$$\mathcal{G} = (1 + 3\,Ri)^{-2} \qquad \text{for} \quad Ri > 0$$
$$\mathcal{G} = (1 - 3\,Ri)^2 \qquad \text{for} \quad Ri \le 0. \tag{3}$$

Mixing length l is according to Blackadar computed as:

$$l = \frac{\kappa(x_2 + y_0)}{1 + \kappa \frac{(x_2 + z_0)}{l_\infty}}, \qquad l_\infty = \frac{27\,|V_g|\,10^{-5}}{f}, \tag{4}$$

where κ is von Karman constant, f marks Coriolis parameter considered as a constant in computed domain: $f = 1.1 \cdot 10^{-4}\,\text{rad.s}^{-1}$, z_0 is surface roughness parameter (choose as tenth of barrier height h), l_∞ means mixing length for $x_2 \to \infty$ and V_g is geostrofic velocity on the top of boundary domain.

2.3. Vegetation model

The vegetative barrier was modelled by adding volume force T, which simulates the aerodynamic resistance caused by the vegetation:

$$T_i = r_h |U| u_i, \tag{5}$$

here $|U|$ is the velocity magnitude and r_h is an obstructing coefficient of the vegetative barrier. The profile for the coefficient was chosen as rhombus, which simulate the distribution of the tree mass and its ability to obstruct the flow:

$$r_h(z) = \begin{cases} r\,\frac{x_2/h}{0.75} & \forall(x_2/h); \quad 0 \le x_2/h \le 0.75 \\ r\,\frac{1 - x_2/h}{1 - 0.75} & \forall(x_2/h); \ 0.75 \le x_2/h \le 1.0, \end{cases} \tag{6}$$

where $r \in \langle 0; 1 \rangle$ is obstructing constant, which characterizes the type of vegetation (0 means no barrier). Different values of these constants have been tested.

2.4. Equation for dust concentration

The contaminant is a non-hygroscopic, primary emitted dust which can be considered as passive scalar in the flow field. The transport of concentration C is described by the advection equation:

$$\frac{\partial \rho C}{\partial t} + \frac{\partial(\rho u_i C)}{\partial x_i} = Z \qquad (7)$$

where Z is source term placed on the highway. The diffusion (in general turbulent) of dust concentration is neglected.

Using second equation of system (1) and some assumptions for Boussinesq approximation the last equation can be rewriten as:

$$\frac{\partial C}{\partial t} + \frac{\partial(u_i C)}{\partial x_i} - u_2 \frac{\partial \rho_0}{\partial x_2} C = \frac{Z}{\rho_0} \qquad (8)$$

When neutral stratification is assumed, the term with $\frac{\partial \rho_0}{\partial x_2} = 0$.

2.5. Vector form of equations

The whole system of governing equations can be rewritten in vector 2D conservative form:

$$PW_{,t} + H(W)_{,x_i}^{(i)} - \nu(R(W)_{,x_i}^{(i)}) = F_{ext}, \qquad (9)$$

where the $W = [p, \rho, u_1, u_2, C]^T$ is vector of unknowns, matrix $P = diag[0, 1, 1, 1, 1]^T$, symbol $(.)_{,x_i}$ or $(.)_{,t}$ denotes derivative, matrices H contain the inviscid fluxes:

$$
\begin{aligned}
H^{(1)} &= [u_1, u_1\rho', u_1^2 + p'/\rho_*, u_1 u_2, u_1 C]^T \\
H^{(2)} &= [u_2, u_2\rho', u_1 u_2, u_2^2 + p'/\rho_*, u_2 C]^T,
\end{aligned}
\qquad (10)
$$

matrices R are the viscous fluxes

$$
\begin{aligned}
R^{(1)} &= [0, 0, u_{1,x_1}, u_{2,x_1}, 0]^T \\
R^{(2)} &= [0, 0, u_{1,x_2}, u_{2,x_2}, 0]^T
\end{aligned}
\qquad (11)
$$

and vector F_{ext} is the source term:

$$
F_{ext} = [0, -u_2\frac{\partial \rho_0}{\partial x_2}, 0, -\frac{\rho'}{\rho_*}g, Z/\rho_0]^T \qquad (12)
$$

3. Numerical approximation

The high resolution finite volume method was used. Discretization was done by the methods of lines.

3.1. Spatial discretization

The AUSM scheme was used for space discretization of inviscid fluxes:

$$\int_{\partial\Omega} [H^{(1)}n_1 + H^{(2)}n_2]ds \approx \qquad (13)$$

$$\approx \sum_{l=1}^{4} \left[\begin{pmatrix} 1 \\ \rho \\ u_{1+/-} \\ u_{2+/-} \\ C_{+/-} \end{pmatrix} u_n + \frac{p}{\rho_*} \begin{pmatrix} 0 \\ 0 \\ n_1 \\ n_2 \\ 0 \end{pmatrix} \right] s_l, \qquad (14)$$

where quantities p and ρ on the cell face are approximated by the central formula from neighbouring cells. Velocities on the cell face are computed using MUSCL reconstruction according to van Leer [4]:

$$u_+ = u_{k+1} - \frac{1}{2}\delta_+, \quad \text{resp.} \quad u_- = u_k + \frac{1}{2}\delta_- \tag{15}$$

with the Hemker-Koren slope limiter function:

$$\delta_{+/-} = \frac{a_{+/-}(b_{+/-}^2 + 2) + b_{+/-}(a_{+/-}^2 + 1)}{2a_{+/-}^2 + 2b_{+/-}^2 - a_{+/-}b_{+/-} + 3}, \tag{16}$$

$$
\begin{aligned}
a_+ &= u_{P+1} - u_P; \ a_- = u_{L+1} - u_L, \\
b_+ &= u_P - u_{P-1}; \ b_- = u_L - u_{L-1}.
\end{aligned}
\tag{17}
$$

The numbers $P, L \in \mathbf{Z}$ denote index values of the velocities (e.g. face between cells (k) and $(k+1)$ i.e $P = k+1$ (index by u_+) a $L = k$ (index by u_-)). The concentration is approximated by simple up-stream method.

Since the pressure is approximated by central difference, the scheme has to be stabilised by the artificial pressure diffusion introduced in [5]. The discrete version of the additional flux i.e. for face between cells (k) and $(k+1)$ is given by:

$$H^{(p)} = [\frac{p_{k+1} - p_k}{\beta_p}, 0, 0, 0, 0]^T, \tag{18}$$

where $\beta_p = U_{max} + \frac{2\nu}{\Delta}$, Δ is the step size of grid. The viscous fluxes are discretized in the central way on dual (diamond type) mesh. This scheme is of the second order in space. See details in [6].

3.2. Time integration

After the space discretization the time derivative is approximated by the robust second order BDF formula. The time step Δt can be chosen according to the problem. If we define the reziduum as:

$$
\begin{aligned}
\text{Rez}(W^{n+1}) := P\frac{3W^{n+1} - 4W^n + W^{n-1}}{2\Delta t} + \\
+ H(W^{n+1}) + R(W^{n+1}) - F_{ext}(W^{n+1}),
\end{aligned}
\tag{19}
$$

then the following system of equations has to be rewritten for the time step $n + 1$:

$$\text{Rez}(W^{n+1}) = 0. \tag{20}$$

This equation is solved by principle of artificial compressibility method in an artificial (dual) time τ. The dual time derivative of pressure is added to the continuity equation. The stationary solution of the following system is sought:

$$\tilde{P}W_{,\tau} + \text{Rez}(W^{n+1}) = 0, \tag{21}$$

where $\tilde{P} = [1, 1, 1, 1]^T$. The system of ODEs is solved by an explicit 3-stage Runge-Kutta method.

4. Validation

The Validation of the model was done on case solved by Bodnar [3]. There were study lee waves generates over the hill. The wavelength of lee waves was compared to the theoretical values and the profiles of vertical velocity on sectional line were compared to the ones within the original article, for validation of the numerical model results.

4.1. Wavelength

The theoretical values of wavelength were computed from the Brunt-Vaisala frequency for each stratification. Than the wavelength was measured by two methods: the distances of the wave maxima were determined and the wavelengths in section line perpendicular to the direction of waves propagation were plotted. The results are shown in Table 1. Considering the errors in measurement (approx. 1 m), the values are in a good agreement.

Table 1. The comparison of theoretical and measured values of wavelength

	Theory	Measure	
		Distance	Section line
$|g|$ $\left[\frac{m}{s^2}\right]$	wavelength [m]		
5	31	33	33
10	22	23	17
20	15	17	12
50	10	10	7

4.2. Vertical velocity profile

The values of vertical velocity were plotted along the sectional line started in the middle of the hill and the inclination was 45 degrees. The plotting was done for each stratification and it was compared to vertical velocities profile from [3]. The amplitudes and the shape of results in Fig. 1 are similar to the original ones in Fig. 2.
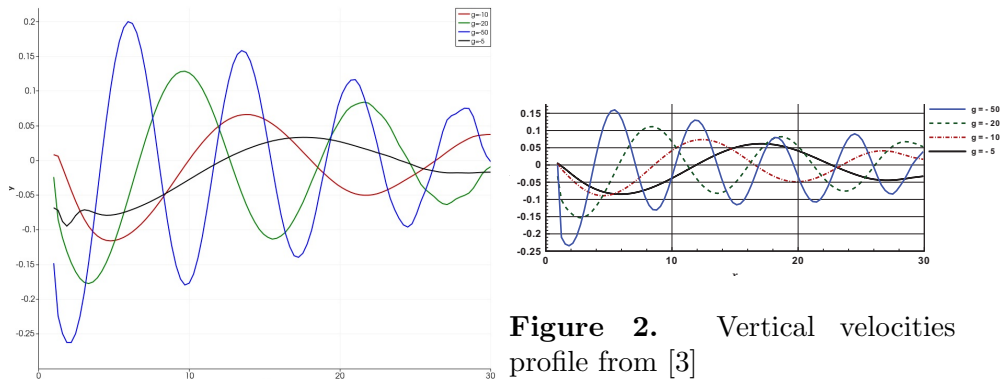

Figure 1. Vertical velocities profiles

Figure 2. Vertical velocities profile from [3]

The lee waves are observed in both figures, there are more waves for higher gravity acceleration in the original figure. It can be caused by a little bit different time of evaluation. Even if there is declared to have the final (stationary) flow in the original figure, the flow is changing a little bit all time and the waves are slightly moving.

5. The numerical experiment and setup

The computational domain was 300×150 m large, the highway is situated in position $x_1 \in \langle 20, 45 \rangle$ m. The vegetative barrier of height $h = 15$ m is located in position $x_1 \in \langle 50, 80 \rangle$ m. Dust source was situated to the center of the highway $x_1 = 32$ m. The source term was set to $Z/\rho_0 = 1$ for all time.

The vertical gradient of the density was $\frac{\partial \rho_0}{\partial x_2} = 0$ as was mentioned before. It matches to homogeneous stratification (can be neutral stratification if the assumption of negligible heat transfer is satisfied). Some other parameters were: $g = -10 \; \frac{m}{s^2}$, kinematic viscosity of air $\nu = 10^{-5} \; \frac{m^2}{s}$.

The structured net consist of 120×300 orthogonal cells. Step in x-direction is equidistant. The vertical step is till height 50 m exponentially diluted, with expansion factor 1.038615706, above 50 m is equidistant with 2 m step. The smallest step is 0.1464334293 m high in x_2-direction (designates in experiments for clarity y-direction).

5.1. Boundary conditions

The boundary conditions were realised by ghost cells method. The values of the unknowns were calculated through the linear extrapolation to obtain the right values on the boundaries.

Inlet: The horizontal velocity component was prescribed by logaritmic wind profile near surface $u_1 = U_{max} \ln(\frac{x_2 - z_0}{z_0})$, over 20 m high it was constant $u_1 = U_{max} = 5 \; \frac{m}{s}$. The homogeneous Dirichlet condition was prescribe for other variables, only the pressure was extrapolated.

Outlet: Homogeneous Neumann condition was prescribed for all variables, only the pressure perturbation was set to 0 Pa.

Top: The perturbation of pressure and density were extrapolated, the velocity component were the same as on inlet top boundary (Dirichlet condition)

Bottom: The perturbation of pressure was extrapolated. The no-slip (homogeneous Dirichlet) condition for velocity components was prescribed and the homogeneous Neumann condition for the density (its perturbation) was given.

6. Results

Three effect of the flow were study. First experiment compared the simple flow (without turbulent model) with turbulent flow. Second one observed the influence of the obstructing constant on the horizontal velocity in 10 m high and the third one study the influence of the obstructing constant on the concentration of dust behind the vegetative barrier.

6.1. The effect of the turbulence model

Two different types of the flow were computed for the obstructing constant $r = 0.3$. First one without turbulent model (ν_T was set to 0) and the second one with it. The results is shown in Figs. 8 and 4. The flow without turbulent model is unsteady, the vortex street was regularly created behind the barrier. Unlike the flow with turbulent model, which is steady, because all vortexes are damped by the turbulent viscosity.

6.2. The influence on the flow

Several situations were computed for different obstructing constants. The horizontal components of velocities were plotted together on sectional line for each situations. The result shows Fig. 5. The breaking effect of the barrier is evident - for higher r is the effect bigger.

The red line shows the situation, when $r = 0.0$, it means the case without any barrier. No breaking effect appeared for this line. However the current at the same high is slowing. The explanation can be in grown boundary layer, turbulent viscosity draw kinetic energy and
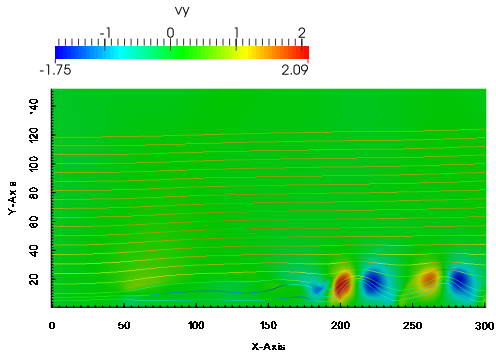
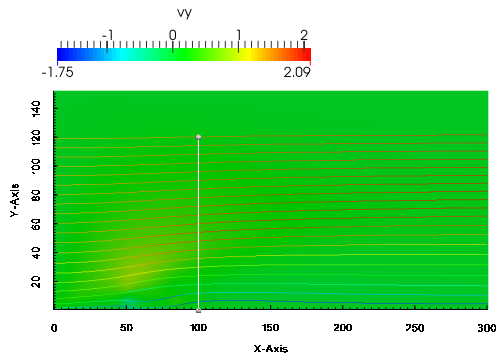**Figure 3.** Vertical velocity and streamlines for $\nu_T = 0$

Figure 4. Vertical velocity and streamlines with turbulent model

the vertical component of velocity is decreasing. For the grow of boundary layer see figure in appendix.

The rapid increase away from the barrier (behind $x = 90$ m) is caused probably by the higher velocity of fluid in lower levels. These levels were not slows so well, because of the obstructing profile, which is lower in lower levels (see Eq. (6)).
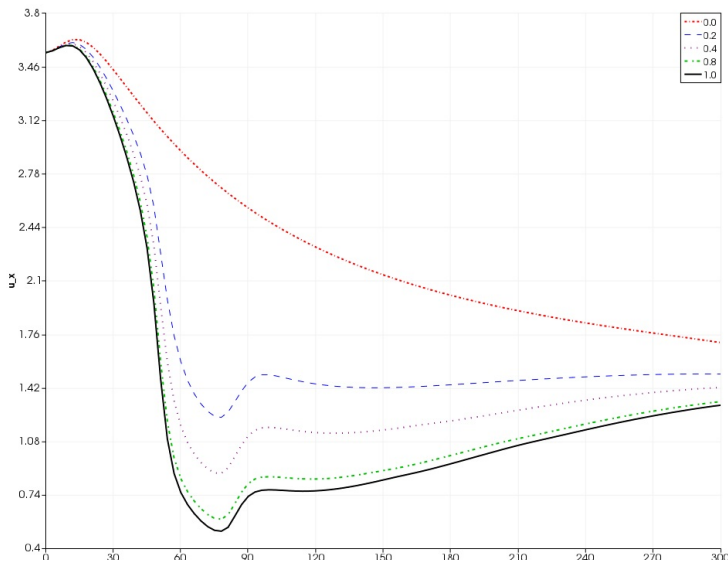

Figure 5. Vertical velocities on sectional line in 10 m height

6.3. The influence on the concentration

The last experiment was pointed on concentration. The concentration were plotted on sectional line placed in points $x = 120$ and $x = 150$ m for the same situations as in previous subsection. The results shows Figs. 6 and 7. The influence of r is apparent. For higher r the maximum of concentration is in higher levels. This should be promising for the human health, but this effect can be weakened with turbulent diffusivity (neglected in this model), with other stratification or with dust sedimentation (also neglected in this model).
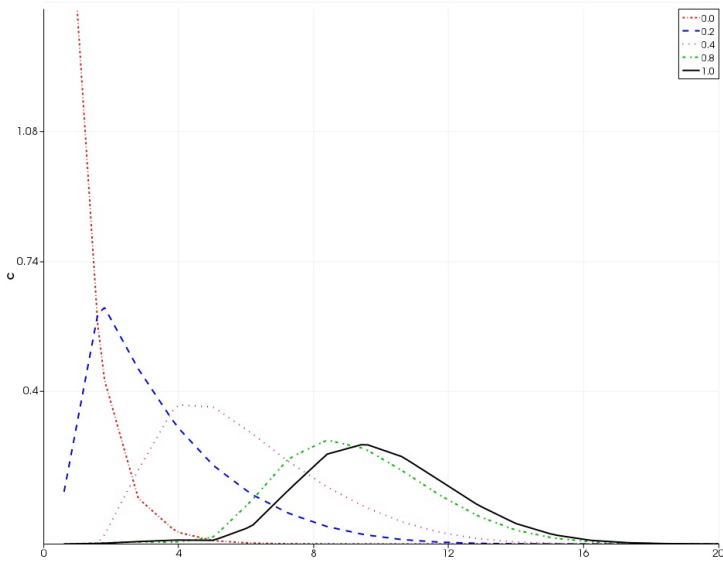
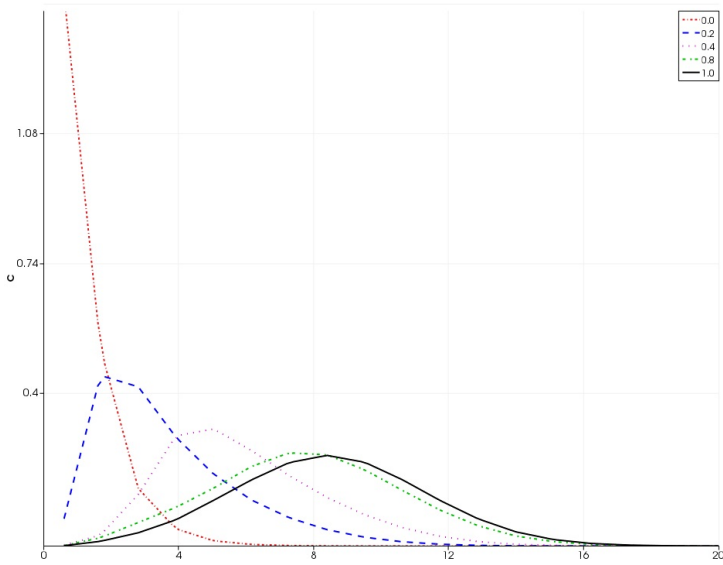**Figure 6.** Concentrations for different r in $x = 120$ m

Figure 7. Concentrations for different r in $x = 120$ m

7. Conclusions

It manage to show influence of vegetative barrier near highway on the flow and the dust concentration. The effect are visible and interesting even for a simple model. However there is a lot of space, how can be this model improved. For example better validation will be needed, if the measurement on highway is done. Turbulent diffusivity of concentration can be added, the dust sedimentation can be added etc.
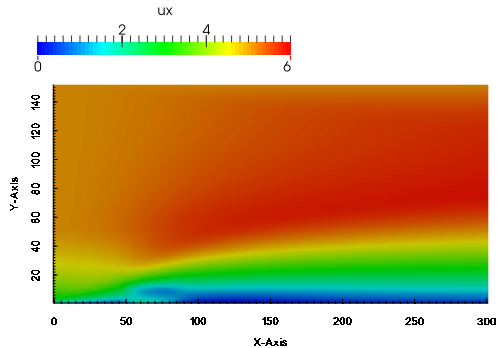
Appendix

Figure 8. Horizontal velocity field
for $r = 0.3$

References

[1] Arya, P.S., 2001, *Introduction to Micrometeorology* , San Diego: Academic press

[2] Blackadar, A.K., 1962, "The Vertical Distribution of Wind and Turbulent Exchange in a Neutral Atmosphere", *J. Geophys. Res.*, vol 67

[3] Bodnar, T., et. al, 2011, "Application of Compact Finite-Difference Schemes to Simulations of Stable Stratified Fluid Flows", *J of Applied Matematics and Computation*, Vol. 08, pp 58

[4] Van Leer, B., 1979, "Towards the Ultimate Conservative Difference Scheme. V. A Second-order Sequel to Godunov's Method",*J. of Computational Physics*, Vol. 32

[5] Dick, E., Vierendeels, J., Riemslagh, K., 1999, "A Multigrid Semi-implicit Line-method for Viscous Incompressible and Low-Mach-number Flows on High Aspects Ratio Grids, *J. of Comp. Physics*, Vol. 154

[6] Ferziger, J. H., Peric, M., 1997, *Computational Methods for Fluid Dynamics*, Springer (2nd edition)